Journal of Applied Electrochemistry (2005) 35:235–241
DOI 10.1007/s10800-004-6309-2

Interactions of polypyridyl cobalt complexes with DNA studied by rotating electrode methods

HONG LI[1,2], ZHENGHE XU[1,3,*], LIANG-NIAN JI[2] and WEI-SHAN LI[1]
[1]*Department of Chemistry, South China Normal University, Guangzhou 510631, P R China*
[2]*Department of Chemistry, Zhongshan University, Guangzhou 510275, P R China*
[3]*Department of Chemical and Materials Engineering, University of Alberta, Edmonton, AB, Canada, T6G 2G6*
*(*author for correspondence, e-mail: zhenghe.xu@ualberta.ca)*

Received 1 April 2004; accepted in revised form 5 October 2004

Key words: DNA, polypyridyl cobalt complex, rotating ring-disk electrode

Abstract

The interaction of transition metal complexes $Co(phen)_2TATP^{3+}$, $Co(phen)_3^{3+}$ and $Co(bpy)_3^{3+}$ (where TATP = 1,4,8,9-tetra-aza-trisphenylene, phen = 1,10-phenanthroline, and bpy = 2,2′-bipyridine) with calf thymus DNA was investigated using the rotating ring-disk electrode technique. The values of the apparent diffusion coefficient and rate constant at the formal potential for reduction of these three polypyridyl cobalt complexes were found to decrease significantly in the presence of DNA as compared with that in the absence of DNA. The formal potentials at which the redox reaction takes place in the absence or presence of DNA were in the order of $Co(phen)_2TATP^{3+/2+} > Co(phen)_3^{3+/2+} > Co(bpy)_3^{3+/2+}$. The interaction between the complexes and DNA varied significantly, depending on the nature of ligands. The binding strength of these complexes to DNA was found in the order of $Co(phen)_2TATP^{3+} > Co(phen)_3^{3+} > Co(bpy)_3^{3+}$. The interaction modes of the polypyridyl cobalt complexes with DNA were discussed in line of electrochemical observations.

1. Introduction

Many metal complexes have the potential to be developed into novel probes of DNA structure [1–5], and can be used as mediators of duplex DNA cleavage reactions [6–8], as anticancer drugs [9] that control the reproduction of DNA in the body of living organs, as electron acceptors and donors for studying long-range electron transfer through DNA films [10–12], as hybridization indicators for DNA electrochemical biosensors [13–21], and as agents for DNA emission labels [22], just to name a few. In the last decades increasing efforts have been devoted to studying the interactions of metal complexes with double-stranded DNAs. The techniques widely used include viscosity and X-ray crystallographic measurements. Spectroscopic methods such as electronic absorption spectroscopy, fluorescence spectroscopy, surface-enhanced Raman scattering, H^1NMR spectroscopy and, more recently, atomic force microscopy also found their role in this important area [23–26]. In comparison, electrochemical methods have so far received little attention for investigating interactions of small molecular complexes with DNAs. Bard et al. [27] demonstrated electrochemical methods to be useful tools to study the binding of metal complexes to DNA. With electrochemical methods, detailed information on the nature of binding metal complexes with DNAs can be obtained by analyzing electrochemical peak current and peak potential. The interaction of some metal complexes, e.g. Co(III) [27–29], Fe(II) [27, 30], Ru(II) [31], Cu(II) [31–32], and Os(II) [33] chelates with 1,10-phenthroline and 2,2′-bipyridine bound to DNA has been investigated by cyclic voltammetry and differential pulse voltammetry or electrogenerated chemiluminescence. From the measured cyclic voltammgrams, the binding properties were interpreted in terms of the interplay of electrostatic interactions of metal complexes with the charged sugar-phosphate back bones and intercalative interactions within the DNA helix (i.e., the stacked base pairs). Thorp et al. [34–37] investigated the electrocatalytic oxidation of guanine and sugar in DNA by oxidizing metal complexes such as ruthenium(III) and oxoruthenium(IV) complexes and their para-substituted derivatives. In a spectroscopic study of $Co(phen)_2TATP^{3+}$ interacting with a DNA (where TATP represents 1,4,8,9-tetra-aza-trisphenylene), the intercalation of TATP ligand into the base pairs of the double stranded DNA has been proposed [38].

In this work, we further extended electrochemical techniques by incorporating rotating ring-disk electrode measurement to investigations of electrochemical characteristics of the redox couples, such as $Co(bpy)_3^{3+/2+}$, $Co(phen)_3^{3+/2+}$ and $Co(phen)_2TATP^{3+/2+}$ in the absence or presence of calf thymus DNA. Use of the

rotating ring-disk electrode measurement allowed us to determine several important parameters such as apparent diffusion coefficient, collection efficiency and redox reaction rate constant at the formal potential in the absence or presence of the DNA. The results provided us with insights on interactions between the metal complexes and DNA for better understanding of their interaction mode and mechanism.

2. Experimental

2.1. *Materials*

All the solutions were prepared with double-distilled water and reagent grade chemicals purchased from commercial vendors and used without further purification. A supporting electrolyte buffer solution was prepared to contain 50 mmol dm^{-3} NaCl and 10 mmol dm^{-3} Tris (where Tris = tris(hydroxy methyl) amino-methane) at the solution pH of 7.0, adjusted with HCl. The double stranded DNA was purchased from Shanghai chemical company. The DNA solution of ca.10^{-5} mol dm^{-3} concentration in a supporting electrolyte solution exhibited two distinct UV absorption bands at 260 and 280 nm. The peak ratio of these two bands is ca. 1.84, indicating that the DNA was sufficiently free of protein [39]. DNA concentration, more precisely nucleotide phosphate (NP) concentration, was determined by UV absorbance at 260 nm. The extinction coefficient was taken to be 6600 mol^{-1} cm^2 [40]. Stock DNA solutions were stored at 4 °C and used within 4 days.

Cobalt complexes with three polypyridyl ligands of increasing aromatic ring (i.e., $Co(bpy)_3Cl_3$, $Co(phen)_3Cl_3$, and $Co(phen)_2TATPCl_3$) were studied. These compounds were prepared according to the procedures reported previously [38, 41]. The chemical structures of the ligands are shown in Figure 1.

2.2. *Instrumentation*

Ultraviolet–visible spectra were obtained using a UV spectrophotometer (Model 240, Shimadzu Corporation, Japan). Rotating ring-disk electrode measurements were conducted using an AFRDE4E double potentiostat/galvanostat (Pine Instrument Company) connected to a Model 3036 X-Y recorder. An AFDT06 gold ring-gold disk electrode matched with AFASR2E analytical rotator was donated by Pine Instrument Company. The Au disk and the Au ring electrodes were moulded in polytetrafluoroethylene separately, resulting in an insulating gap of 0.16 mm between the electrodes. The radius for the disc (r_1), insulating gap (r_2) and the ring (r_3) were 3.825, 3.985, and 4.215 mm, respectively. The theoretical value of the collection efficiency for the Au–Au electrode was 0.179 calculated from geometry, which is in good agreement with the experimental value of 0.179 ± 0.001 determined from the current–potential relationship in the solution containing potassium ferricyanide at various rotation speeds.

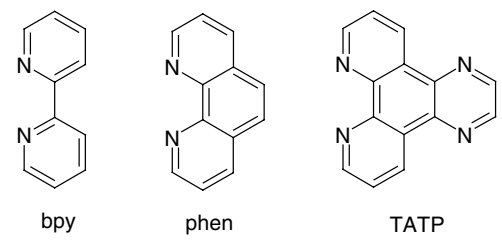

Fig. 1. Structure of ligands 2,2′-bipyridine (bpy), 1,10-phenanthroline (phen) and 1,4,8,9-tetra-aza-trisphenylene (TATP).

2.3. *Procedures*

All the experiments were performed in a single-compartment electrochemical cell of volume 25 ml at room temperatures (25–27 °C), unless otherwise stated. The Au disk–Au ring (A_{disk} = 0.459 cm^2 and A_{ring} = 0.059 cm^2) was used as working electrodes. Prior to each series of measurements the working electrode was polished with 0.25 μm alumina paste on a polishing cloth (Buehler) and then subjected to ultrasonic cleaning for about 10 min in double distilled water. A saturated calomel electrode (SCE) was used as the reference electrode and a Pt flat as the counter electrode. Before each experiment, solutions were deoxygenated by purging with 99.99% N_2 gas for 20 min. During the measurement, a positive N_2 flow was maintained over the solution to ensure an inert atmosphere. To establish experimental errors, a selected number of tests was repeated five times and the variation was found to be within ±3%.

3. Results and discussion

Figure 2 shows current–potential curves of 0.22 mmol dm^{-3} $Co(bpy)_3^{3+}$, $Co(phen)_3^{3+}$ and $Co(phen)_2TATP^{3+}$ obtained in buffered solutions containing different amount of DNA. Curves 1a and 1b in Figure 2 represent the current–potential curve obtained without DNA addition. It is interesting to note a plateau of the limiting current for all the current–potential curves obtained at the ring-disk electrode, suggesting a mass transfer controlled electrochemical reduction of polypyridyl cobalt complexes under sufficiently negative applied potentials. By processing the data using a mixed control model, it is possible to eliminate the effect of concentration polarization and thereby to derive parameters characteristic of mass transfer control and electrochemical control, respectively.

3.1. *Interaction under mass transfer control*

From Figure 2, it can be seen that in the presence of DNA the limiting current plateau value of the current–potential curves decreases markedly with increasing DNA concentration. The difference of limiting current

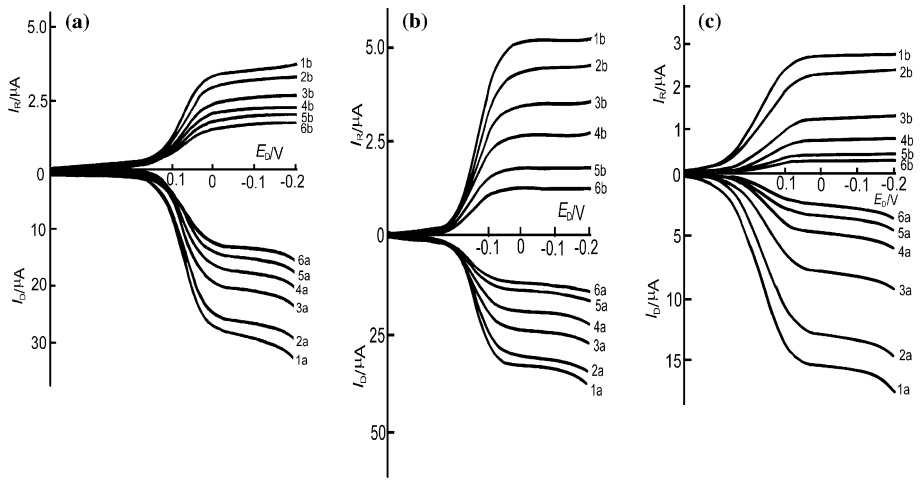

Fig. 2. Disk (I_D) and ring (I_R) currents as a function of the disk potential for 0.22 mmol dm^{-3} $Co(bpy)_3^{3+}$ (a), $Co(phen)_3^{3+}$ (b) and $Co(phen)_2TATP^{3+}$ (c) at Au–Au electrode. Ring potential E_R at 0.2 V and sweep rate of 5 mV s^{-1} with a rotating speed of 10 r s^{-1}. *R* is set at 0 (1), 0.7 (2), 5.0 (3), 10.0 (4), 20.0 (5) and 30.0 (6), respectively.

plateau value in the absence and presence of the DNA can be considered as the degree of redox reaction suppression, which is related to the interaction strength of the DNA with metal complexes. Therefore, this difference is a measure of binding strength of DNA with various metal complexes. For the convenience of discussion, the relative reduction of the limiting current caused by DNA addition, *IS*, is calculated for all three complexes at a DNA addition level of 4.4 mmol dm^{-3} (i.e., $R = 20$, where *R* is defined as the molar concentration ratio of nucleotide phosphate to cobalt(III) complexes). The results in Table 1 show that the binding strength of the DNA with polypyridyl cobalt complexes varies markedly, depending on the nature of the ligands. An increasing order in *IS* from $Co(bpy)_3^{3+}$ to $Co(phen)_3^{3+}$ and finally $Co(phen)_2(TATP)^{3+}$ is observed. This order conforms to the proposed binding mechanism of DNA with the metal complex [42]. Based on this binding mechanism, an increase in planar size and hydrophobicity of the intercalated ligand is anticipated to cause an increase in the overlap of the interposed ligand and base pairs of DNA, which leads to a stronger interaction between the ligand and base pairs. According to molecular structure shown in Figure 1, ligand TATP is anticipated to have the largest overlap with DNA molecules, while bpy has the smallest with phen being in between.

In order to further investigate the strength of DNA interaction with various polypyridyl cobalt complexes, it is instructive to examine the variation of complex diffusion coefficients (*D*) with DNA addition. For this purpose, experiments were carried out with the electrode rotating at different speed (ω). Results obtained without DNA addition in Figure 3 show an increase in limiting current with increasing rotation speed. As shown in Figure 4, the addition of 4.4 mmol dm^{-3} DNA suppressed limiting current at all electrode rotating speeds investigated. For comparison, the limiting current density i_l is plotted against square root of rotational speed $\omega^{1/2}$ in Figure 5 for all three Co-polypridyl complexes without and with DNA addition. It is interesting to note a linear dependence of limiting current on $\omega^{1/2}$ with the straight lines passing through the origin for all the cases investigated. This observation confirms a diffusion controlled electrode process in the current system and the diffusion coefficient can be extracted from the slope of the straight lines. The diffusion coefficients of $Co(bpy)_3^{3+}$, $Co(phen)_3^{3+}$ and $Co(phen)_2TATP^{3+}$ obtained as such in the absence and presence of 4.4 mmol dm^{-3} DNA are summarized in Table 1. Without DNA addition, the diffusion coefficients for $Co(phen)_3^{3+}$ and $Co(bpy)_3^{3+}$ are comparable and significantly higher than that for $Co(phen)_2TATP^{3+}$. This observation is consistent with molecular size consider-

Table 1. Electrochemical parameters from RDE experiments

Complexes	*R*	10^6 *D*/cm^2 s^{-1}	[a]*IS*/%	[b]$E^{\circ\prime}$/V	[c]10^3 k_{fals} ($E^{\circ\prime}$)/cm s^{-1}
$Co(bpy)_3^{3+}$	0	4.7	47.5	0.079	9.1
	20	1.7		0.073	5.0
$Co(phen)_3^{3+}$	0	6.0	59.3	0.135	14.1
	20	1.4		0.146	6.8
$Co(phen)_2(TATP)^{3+}$	0	1.8	80.5	0.170	6.0
	20	0.1		0.168	1.4

[a] $IS/\% = [(i_l)_{R=0} - (i_l)_{R=20}] / (i_l)_{R=0} \times 100\%$.
[b] $E^{\circ\prime} = (E_{p,a} + E_{p,c})/2$, the values of $E_{p,a}$ and $E_{p,c}$ were obtained from cyclic voltammograms.
[c] k_f ($E^{\circ\prime}$) was taken as the rate constant at formal potential, $E^{\circ\prime}$.

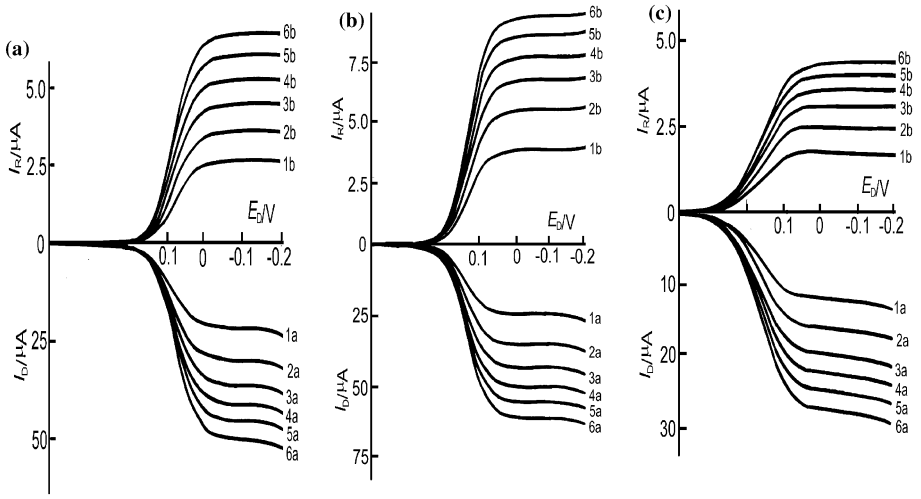

Fig. 3. Polarization curves at Au–Au electrode in the buffered solution containing 0.22 mmol dm^{-3} $Co(bpy)_3^{3+}$ (a), $Co(phen)_3^{3+}$ (b) and $Co(phen)_2TATP^{3+}$ (c) at $E_R = 0.2$ V and sweep rate of 5 mV s^{-1}. Rotating speed (r s^{-1}) is set at 5 (1), 10 (2), 15 (3), 20 (4), 25 (5), and 30 (6), respectively.

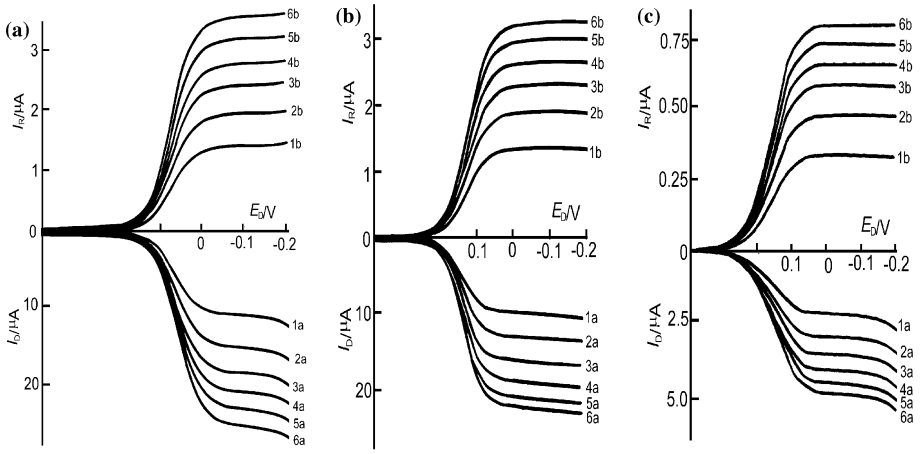

Fig. 4. Polarization curves at Au–Au electrode in the buffered solution containing 4.4 mmol dm^{-3} DNA and 0.22 mmol dm^{-3} $Co(bpy)_3^{3+}$ (a), $Co(phen)_3^{3+}$ (b) and $Co(phen)_2TATP^{3+}$ (c) at $E_R = 0.2$ V and sweep rate of 5 mV s^{-1}. Rotating speed (r s^{-1}) is set at 5 (1), 10 (2), 15 (3), 20 (4), 25 (5), and 30 (6), respectively.

ation of the ligands, with the largest TATP exhibiting the lowest diffusion coefficient. Results also demonstrate that DNA addition resulted in a significant decrease in diffusion coefficient with the relative reduction of diffusion coefficient in the order of $Co(phen)_2TATP^{3+}$ > $Co(phen)_3^{3+}$ > $Co(bpy)_3^{3+}$. We believe that the decrease in diffusion by DNA addition is largely caused by the increased molecular weight of the active species coupled with DNA [27].

In order to better understand what was occurring on the Au disk electrode surface, the collection experiment was performed to measure the current on the Au ring electrode with the potential maintained at a given value. When the potential of the ring was held at 0.2 V, reduction products formed on the disk were swept over by the radial flow streams to the ring where they were collected and oxidized. From the polarization curves of rotating Au–Au electrode, collection efficiency (N), defined as the ratio of the ring current plateau to the disk current plateau can be determined. In this study, the N values for the reduction products of $Co(bpy)_3^{3+}$, $Co(phen)_3^{3+}$ and $Co(phen)_2TATP^{3+}$ cations are determined as a function of DNA concentration and the results are given in Table 2. Also included in this table is the ratio of the experimentally-determined to the theory-based collection efficiencies, which is designated as desorption efficiency (DE) of the reduction products. A lower DE defined as such represents a system of less reduction products transfer from the disk electrode to the ring electrode. In this case, some of the reduction products adsorbed on the rotating disk electrode are unable to move to the ring electrode. Such a system characterizes a stronger adsorption of the reduction product on the disk electrode. Therefore, the magnitude of the DE can be used to measure the adsorption strength of electrochemical reaction products. Based on this definition, the results of the collection efficiency and DE in Table 2 show that the DNA addition caused a significant reduction in both collection and desorption efficiencies for $Co(phen)_3^{3+}$

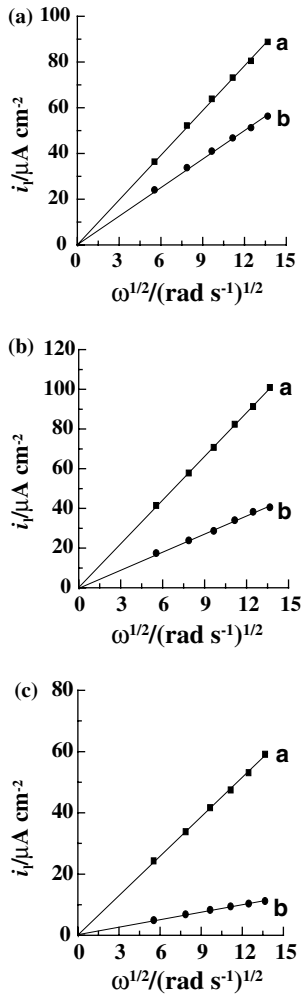

Fig. 5. Dependence of limiting current density (i_l) for the reduction of 0.22 mmol dm^{-3} $Co(bpy)_3^{3+}$ (a), $Co(phen)_3^{3+}$ (b) and $Co(phen)_2TATP^{3+}$ (c) on the rotating speed at $R = 0$ (square) and $R = 20$ (circle) with $E_R = 0.2$ V and sweep rate of 5 mV s^{-1}.

and $Co(phen)_2TATP^{3+}$. For $Co(bpy)_3^{3+}$, both the collection and desorption efficiencies remained the same. This intriguing observation can be explained by a relatively weaker interaction of DNA with $Co(bpy)_3^{3+}$ than with $Co(phen)_3^{3+}$ and $Co(phen)_2TATP^{3+}$ as proposed from the above Au–Au rotating electrode polarization studies shown in Figure 2. The interaction of DNA with $Co(bpy)_3^{3+}$, forming a complex of less positive charges, is of an electrostatic nature, as has been generally acknowledged [43, 44]. However, such an interaction mechanism appears to be not the case for the other complexes. As suggested previously [38, 43], ligands TATP of $Co(phen)_2TATP^{3+}$ and phen of $Co(phen)_3^{3+}$ can intercalate partially into DNA and overlap with the base pairs of DNA molecules. As a consequence, the molecular weight of the reactants and products is anticipated to increase. The decreased collection efficiency and DE of the electrochemical reduction products can thus be rationally explained by their increased molar mass.

Finally, it is worth mentioning that the rotation speed has a relatively small impact on collection coefficient as seen from the results in Table 3. The implication is that the reduction products of $Co(bpy)_3^{3+}$, $Co(phen)_3^{3+}$ and $Co(phen)_2TATP^{3+}$ on gold electrode, whether they exist in a single complex or compounded with DNA, may be rather stable in the solution.

3.2. *Interaction under electrochemical control*

Rate constants of the electrochemical reduction reactions of $Co(bpy)_3^{3+}$, $Co(phen)_3^{3+}$ and $Co(phen)_2TATP^{3+}$ at formal potentials can be derived from the experimental results obtained using the ring-disk elec-

Table 2. Collection (N) and DE (DE) as a function of R (R = [NP]/[polypyridyl cobalt complex])

Complexes		R					
		0	0.7	5.0	10.0	20.0	30.0
$Co(phen)_2TATP^{3+}$	N	0.16	0.15	0.15	0.14	0.12	0.11
	DE/%	91.1	85.5	82.7	80.4	69.8	59.8
$Co(phen)_3^{3+}$	N	0.15	0.14	0.14	0.14	0.13	0.11
	DE/%	82.7	79.3	78.8	77.1	72.1	60.9
$Co(bpy)_3^{3+}$	N	0.12	0.12	0.12	0.12	0.12	0.12
	DE/%	69.8	69.8	68.7	67.0	67.6	67.0

Table 3. Collection efficiency (N) as a function of rotation rate (f)

Complexes		f/Hz					
	R	5	10	15	20	25	30
$Co(bpy)_3^{3+}$	0	0.12	0.12	0.13	0.12	0.13	0.13
	20	0.12	0.12	0.12	0.12	0.13	0.13
$Co(phen)_3^{3+}$	0	0.15	0.15	0.15	0.15	0.15	0.15
	20	0.13	0.13	0.13	0.13	0.13	0.13
$Co(phen)_2TATP^{3+}$	0	0.16	0.16	0.16	0.16	0.16	0.16
	20	0.12	0.13	0.12	0.13	0.12	0.13

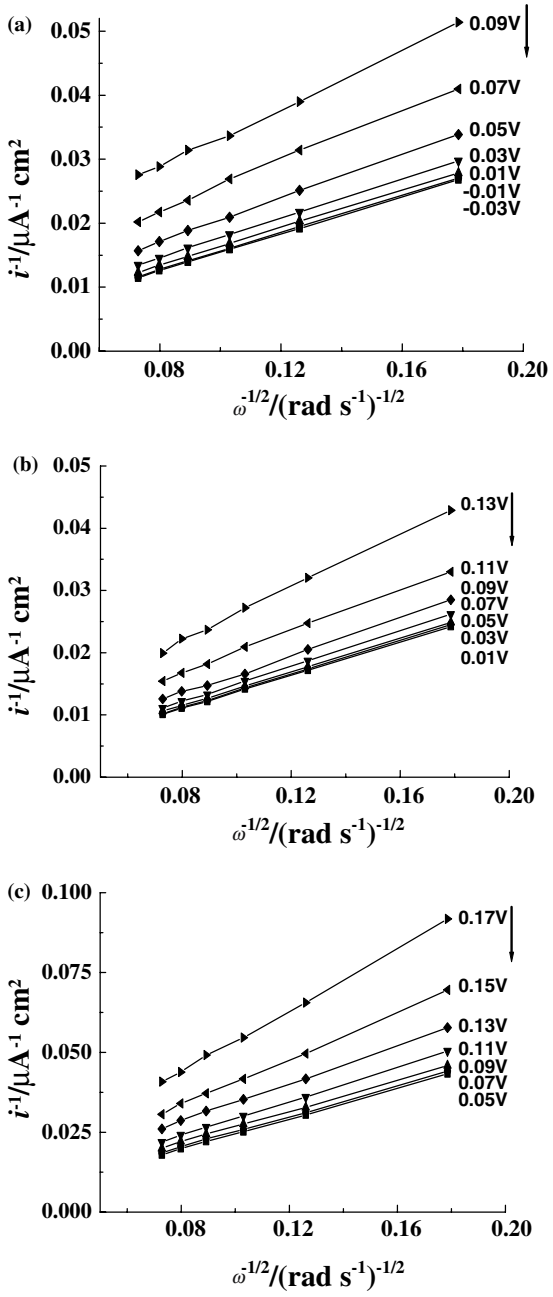

Fig. 6. Plot of i^{-1} against $\omega^{-1/2}$ for $Co(bpy)_3^{3+}$ (a), $Co(phen)_3^{3+}$ (b) and $Co(phen)_2TATP^{3+}$ (c) with the data from Figure 3. Arrows show the negative shift of the selected potential.

trode rotating at various speeds. The results in Figure 2 over the mixed control region were analyzed and a linear plot of i^{-1} against $\omega^{-1/2}$ was obtained as shown in Figure 6. The results can be analyzed using the Levich equation [45],

$$\frac{1}{i} = \frac{1}{i_k} + \frac{1}{0.620nAFC^*D^{2/3}V^{-1/6}\omega^{1/2}} \quad (1)$$

where i_k is kinetic limiting current, n is the number of electrons involved in electrochemical reactions, A is the geometrical area of the disk electrode, C^* is bulk concentration of the reactant, D is diffusion coefficient, v is kinematic viscosity, and ω is electrode rotation speed. According to the Levich equation, the intercept is the reciprocal of i_k. From i_k at a given E, the rate constant, $k_f(E)$ for electrochemical reduction reactions at various potentials can be estimated by the following equation [45]:

$$i_k = nFk_f(E)C^* \quad (2)$$

According to the theory of electrochemical kinetics [45], the $k_f(E)$ at a given potential E can be related to the electrochemical rate constant at the standard electrochemical potential, k_f^0 by

$$k_f = k_f^0 \exp[-\alpha F(E - E^\circ)/RT] \quad (3)$$

where E° is the standard potential of the electrochemical reactions, and α is the charge transfer coefficient. If the formal potential ($E^{\circ\prime}$), taken as a half of the sum of oxidation ($E_{p,a}$) and reduction ($E_{p,c}$) peak potentials (i.e., $E^{\circ\prime} = (E_{p,a} + E_{p,c})/2$) [27], is substituted for E° in Equation 3, the pre-exponent factor becomes the rate constant at formal potential, $k_f(E^{\circ\prime})$. Equation 3 then becomes

$$k_f = k_f(E^{\circ\prime})\exp[-\alpha F(E - E^{\circ\prime})/RT] \quad (4)$$

In Equation 4, $E^{\circ\prime}$ represents the formal potential for the reaction of corresponding $Co(bpy)_3^{3+/2+}$, $Co(phen)_3^{3+/2+}$ and $Co(phen)_2TATP^{3+/2+}$ couples. Their values given in Table 1 are obtained from cyclic voltammograms. The rate constant at $E^{\circ\prime}$ determined from the experimental data for $Co(bpy)_3^{3+}$, $Co(phen)_3^{3+}$ and $Co(phen)_2TATP^{3+}$ without and with 4.4 mmol dm^{-3} DNA addition is also summarized in Table 1.

As shown in Table 1, among the three Co(III)-polypridyl complexes, $Co(phen)_3^{3+}$ exhibited the highest rate constant, indicating that $Co(phen)_3^{3+}$ is the most electrochemically reactive. The addition of DNA decreased the electrochemical reduction rate constants of the aforementioned polypyridyl cobalt complexes. The passivation and blockage by the adsorbed DNA at a gold electrode in the presence of DNA could contribute to the low electrochemical reduction rate constants. More importantly, the electrostatic interaction between the positively charged $Co(bpy)_3^{3+}$ and negatively charged DNA reduces the positive charge density of the active species. As a result, the electrostatic attraction of reactant to the electrode is reduced, resulting in a concentration decrease of the reactant in the reaction layer as predicted by the well known Boltzmann distribution. In the case of $Co(phen)_3^{3+}$ and $Co(phen)_2TATP^{3+}$, the intercalation or groove binding action also contributes, to a considerable extent, to the increase in the reduction reaction resistance also due to the reduced positive charge. This additional binding action accounts for a much more significant relative reduction in the

reduction reaction rate constant by DNA addition for $Co(phen)_3^{3+}$ and $Co(phen)_2TATP^{3+}$ than for $Co(bpy)_3^{3+}$

4. Conclusions

The rotating ring-disk electrode technique was demonstrated to be a viable method to study the interactions of metal complexes with biomacromolecules, such as calf thymus DNA. From this study, the following conclusions are derived.

1. The binding strength of DNA with polypyridyl cobalt complexes is in the order of $Co(phen)_2TATP^{3+} > Co(phen)_3^{3+} > Co(bpy)_3^{3+}$.
2. DNA addition caused a significant decrease in the values of the apparent diffusion coefficient of the three complex cations under diffusion control, and the reduction reaction rate constant at formal potential of the three polypyridyl cobalt complexes under the electrochemical control conditions.
3. In the presence of DNA significant differences exist in the collection and desorption efficiency of the reduction products of $Co(bpy)_3^{3+}$, $Co(phen)_3^{3+}$ and $Co(phen)_2TATP^{3+}$, suggesting a different interaction mode. In addition to electrostatic interaction, the intercalation or groove binding may play an important role in the binding of DNA with $Co(phen)_3^{3+}$ and $Co(phen)_2TATP^{3+}$, but not with $Co(bpy)_3^{3+}$.

Acknowledgements

We are grateful to the National Natural Science Foundation of China and the NSF of Guangdong Province for their financial support.

References

1. A.C. Lim and J.K. Barton, *Biochem.* **37** (1998) 9138.
2. J.Z. Wu, H. Li, J.G. Zhang and J.H. Xu, *Inorg. Chem. Commun.* **5** (2002) 71.
3. X.H. Zou, B.H. Ye, H. Li, J.G. Lin, Y. Xiong and L.N. Ji, *J. Chem. Soc. Dalton. Trans.* (1999) 1423.
4. J.G. Liu, B.H. Ye, H. Li, L.N. Ji, R.H. Li and J.Y. Zhou, *J. Inorg. Biochem.* **73** (1999) 117.
5. Z.S. Yang, J.S. Yu and H.Y. Chen, *J. Electroanal. Chem.* **530** (2002) 68.
6. J. Liu, T.B. Lu, H. Li, Q.L. Zhang, L.N. Ji, T.X. Zhang, L.H. Qu and H. Zhou, *Transit. Metal Chem.* **27** (2002) 686.
7. Z.S. Yang, J.S. Yu and H.Y. Chen, *Electroanalysis* **14** (2002) 747.
8. C.A. Detmer, F.V. Pamatong and J.R. Bocarsly, *Inorg. Chem.* **36** (1997) 3676.
9. T.W. Hambley, *J. Chem. Soc. Dalton. Trans.* (2001) 2711.
10. B. Giese, J. Amaudrut, A.K. Kohler, M. Spormann and S. Wessely, *Nature* **412** (2001) 318.
11. F.D. Lewis, X.Y. Liu, J.Q. Liu, S.E. Miller, R.T. Hayes and M.R. Wasielewski, *Nature* **406** (2000) 51.
12. S.O. Kelley and J.K. Barton, *Science* **283** (1999) 375.
13. D.W. Pang, M. Zhang, Z.L. Wang, Y.P. Qi, J.K. Cheng and Z.Y. Liu, *J. Electroanal. Chem.* **403** (1996) 183.
14. A. Erdem, B. Meric, K. Kerman, T. Dalbasti and M. Ozsoz, *Electroanalysis* **11** (1999) 1372.
15. E. Palecek, *Talanta* **56** (2002) 809.
16. T.M. Herne and M.J. Tarlov, *J. Am. Chem. Soc.* **119** (1997) 8916.
17. K. Hu, R. Pyati and A.J. Bard, *Anal. Chem.* **70** (1998) 2870.
18. G. Chiti, G. Marrazza and M. Mascini, *Anal. Chim. Acta.* **427** (2001) 155.
19. M. Aslanoglu, A. Houlton and B.R. Horrocks, *Analyst* **123** (1998) 753.
20. L.J. Yang and T.Z. Peng, *Chinese J. Anal. Chem.* **29** (2001) 355.
21. J. Labuda, M. Buckova, L. Heilerova, S. Silhar and I. Stepanek, *Anal. Bioanal. Chem.* **376** (2003) 168.
22. X.H. Zou, B.H. Ye, H. Li, Q.L. Zhang, H. Chao, J.G. Liu, L.N. Ji and X.Y. Li, *J. Biol. Chem.* **6** (2001) 143.
23. N. Nikolis, C. Methenitis and G. Pneumatikakis, *J. Inorg. Biochem.* **95** (2003) 177.
24. J.G. Collins, A.D. Sleeman, J.R. Aldrich-Wright, I. Greguric and T.W. Hambley, *Inorg. Chem.* **37** (1998) 3133.
25. T.W. Hambley, *J. Chem. Soc. Dalton Trans.* (2001) 2711.
26. J. Wang and A.J. Bard, *Anal. Chem.* **73** (2001) 2207.
27. M.T. Carter, M. Rodriguez and A.J. Bard, *J. Am. Chem. Soc.* **111** (1989) 8901.
28. D.W. Pang and H.D. Abruna, *Anal. Chem.* **70** (1998) 3162.
29. P.T. Selvi and M. Palaniandavar, *Inorg. Chim. Acta* **337** (2002) 420.
30. M. Aslanoglu, C.J. Isaac, A. Houlton and B.R. Horrocks, *Analyst* **125** (2000) 1791.
31. G.C. Zhao, J.J. Zhu and H.Y. Chen, *Chem. Res. Chinese Univ.* **13** (1997) 117.
32. J. Labuda, M. Buckova, M. Vanickova, J. Mattusch and R. Wennrich, *Electroanalysis* **11** (1999) 101.
33. M. Rodriguez and A.J. Bard, *Anal. Chem.* **62** (1990) 2658.
34. B.T. Farrer and H.H. Thorp, *Inorg. Chem.* **39** (2000) 44.
35. V.A. Szalai, J. Jayawickamarajah and H.H. Thorp, *J. Phys. Chem. B.* **106** (2002) 709.
36. M.E. Napier and H.H. Thorp, *J. Fluoresc.* **9** (1999) 181.
37. J. Kim, *Bull. Korean Chem. Soc.* **21** (2000) 709.
38. X.F. He, L. Wang, H. Chen, L. Xu and L.N. Ji, *Polyhedron* **17** (1998) 3161.
39. P.O.P. Ts'o and P. Lu, *Proc. Acad. Sci. USA.* **51** (1964) 17.
40. M.E. Reichmann, S.A. Rice, C.A. Thomas and P. Doty, *J. Am. Chem. Soc.* **76** (1954) 3047.
41. G Grassini-Strazza and M. Sinibaldi, *Inorg. Chem. Acta* **44** (1980) 295.
42. Q.X. Zhen, B.H. Ye, J.G. Liu, L.N. Ji and L. Wang, *Chem. J. Chinese Univ.* **20** (1999) 1661.
43. M.B. Fleisher, K.C. Waterman, N.J. Turro and J.K. Barton, *Inorg. Chem.* **25** (1986) 3549.
44. C.V. Kumar, J.K. Barton and N.J. Turro, *J. Am. Chem. Soc.* **107** (1985) 5518.
45. A.J. Bard and L.R. Faulkner, 'Electrochemical Methods' (John Wiley & Sons, New York, 1980) p. 280.